

Spatial and Temporal Characteristics of Summer Precipitation over Central Europe in a Suite of High-Resolution Climate Models

PETTER LIND, DAVID LINDSTEDT, AND ERIK KJELLSTRÖM

*Swedish Meteorological and Hydrological Institute, Norrköping, and Department of Meteorology, Sweden
Stockholm University, Stockholm, Sweden*

COLIN JONES

*National Centre for Atmospheric Science, University of Leeds, Leeds, United Kingdom, and Swedish
Meteorological and Hydrological Institute, Norrköping, Sweden*

(Manuscript received 3 July 2015, in final form 29 December 2015)

ABSTRACT

High-impact, locally intense rainfall episodes represent a major socioeconomic problem for societies worldwide, and at the same time these events are notoriously difficult to simulate properly in climate models. Here, the authors investigate how horizontal resolution and model formulation influence this issue by applying the HIRLAM–ALADIN Regional Mesoscale Operational NWP in Europe (HARMONIE) Climate (HCLIM) regional model with three different setups: two using convection parameterization at 15- and 6.25-km horizontal resolution (the latter within the “gray zone” scale), with lateral boundary conditions provided by ERA-Interim and integrated over a pan-European domain, and one with explicit convection at 2-km resolution (HCLIM2) over the Alpine region driven by the 15-km model. Seven summer seasons were sampled and validated against two high-resolution observational datasets. All HCLIM versions underestimate the number of dry days and hours by 20%–40% and overestimate precipitation over the Alpine ridge. Also, only modest added value was found for gray-zone resolution. However, the single most important outcome is the substantial added value in HCLIM2 compared to the coarser model versions at subdaily time scales. It better captures the local-to-regional spatial patterns of precipitation reflecting a more realistic representation of the local and mesoscale dynamics. Further, the duration and spatial frequency of precipitation events, as well as extremes, are closer to observations. These characteristics are key ingredients in heavy rainfall events and associated flash floods, and the outstanding results using HCLIM in a convection-permitting setting are convincing and encourage further use of the model to study changes in such events in changing climates.

1. Introduction

In August 2002 central Europe experienced an extreme rainfall episode where a number of flash floods led to record-breaking rainfall amounts (locally up to 300 mm in 24 h), caused several rivers to overflow, and resulted in huge economical loss and a significant number of fatalities (Ulbrich et al. 2003). In the past, central

Europe has frequently been affected by similar precipitation events, often with large socioeconomic impacts (Rotunno and Ferretti 2001; Kundzewicz et al. 2005; Frei et al. 2000; Ruiz-Villanueva et al. 2012). There is also evidence that precipitation extremes have become more common over recent decades (van den Besselaar et al. 2012), and, despite large intermodel differences, there is suggestion of increases in the frequency and/or intensity of extreme precipitation events in Europe in the future, both on daily (e.g., Feldmann et al. 2013; Lenderink and van Meijgaard 2010; Frei et al. 2006; Ban et al. 2015) and subdaily time scales (e.g., Ban et al. 2015; Kendon et al. 2014). Estimates of future changes in extremes of multihourly precipitation sums are critical for risk and impact assessment of changes in frequency of flash floods and major flooding events.

 Denotes Open Access content.

Corresponding author address: Petter Lind, Swedish Meteorological and Hydrological Institute, Folkborgsvägen 17, 601 76 Norrköping, Sweden.
E-mail: petter.lind@smhi.se

DOI: 10.1175/JCLI-D-15-0463.1

A correct representation of these heavy rainfall events is an important (but not sufficient) condition to have confidence in projections for the future.

The concept of flash floods is underpinned by a simple but important statement; the heaviest precipitation occurs where the rainfall rate is the highest for the longest time. Numerical experiments and analysis of observed episodes of heavy rainfall in central Europe reveal a number of common key ingredients. The dynamical and thermodynamical interactions from synoptic to local scales have been just right to enable sufficient moisture convergence and vertical updrafts and hence condensation and rainfall, as well as constraining convective systems to become quasi-stationary (Doswell et al. 1996; Lin et al. 2001). In addition, airflow–orography interactions may modify the development of precipitation-producing storms in critical ways by influencing the low-level stability and convergence patterns (Rotunno and Ferretti 2001). The main characteristics of a flash flood constitute a challenge for weather and climate models, as it requires an accurate representation of the local environment and storm dynamics.

A well-known source of error for the simulation of precipitation in numerical models is the parameterization of convection (Molinari and Dudek 1992; Hohenegger and Stevens 2013; O’Gorman and Schneider 2009). Individual moist convective updrafts and downdrafts have horizontal dimensions on the order of 0.1–10 km. Their role in restabilizing the lower atmosphere through production of clouds and precipitation are critical for a correct and physically sound representation of weather and climate. In large-scale models with mesh-grid sizes of $O(100)$ km the statistical effects of convection on the grid scale are parameterized, but because of this, the convection scheme usually struggles to capture local and regional interactions (e.g., orographically forced convection in steep topography) as well as the detailed temporal evolution of convection at subdaily time scales (e.g., Dai and Trenberth 2004; Dai 2006; Bechtold et al. 2004). Similar problems are seen also in regional climate models (RCMs) with parameterized convection (Liang 2004; Brockhaus et al. 2008). Generally, as the grid mesh becomes finer, the realism of precipitation patterns and intensities improves in models (e.g., Rauscher et al. 2010; Sharma and Huang 2012; Prein et al. 2016; Gao et al. 2006); however, there are still errors in subdaily precipitation statistics even at resolutions of approximately 10 km in models with an active convection scheme (Walther et al. 2013). Originally designed for coarser grids, convection schemes at approximately 10 km begin to violate the underlying statistical assumptions on which they are based; most importantly, the assumption of scale

separation is no longer valid. At even finer resolution, entering the so-called “gray zone” resolution of approximately 3–10 km, the issues of double counting convective precipitation (parameterized and resolved) and excessive gridpoint stabilization (Gerard 2007; Gerard et al. 2009) further degrade the model convective precipitation response.

In convection-permitting models (1–4-km mesh size) there is a much better description of precipitation processes, such as the initiation and organization of convection, orographic enhancement, and small-scale storm characteristics (Prein et al. 2015). In numerical weather prediction (NWP), convection-permitting models (CPMs) are now routinely delivering significantly improved accuracy in quantitative precipitation forecasts (e.g., Weusthoff et al. 2010; Lean et al. 2008; Roberts et al. 2009; Roberts and Lean 2008). In particular, Roberts and Lean (2008) showed that the spatial frequency of precipitation was significantly improved in kilometer-scale simulations compared to coarser ones, particularly for localized, heavy precipitation events. In an excellent review on the use of CPMs in the climate modeling community, Prein et al. (2015) discuss at length the success in improving the simulation of various aspects of precipitation and other meteorological variables referencing a multitude of studies. Recently, Kendon et al. (2012) demonstrated an improved representation of duration and spatial extent of precipitation extremes in a convection-permitting climate model (CPCM) compared to a coarser-scale RCM. Using the same model simulations, but focusing on the statistical behavior of precipitation extremes, Chan et al. (2014) showed that the CPCM was superior to the coarser model in representing summer hourly and multihourly precipitation extremes. Furthermore, the typical deficiencies of a too-early onset and decay of diurnal convective precipitation, as well as too-low peak intensities, in RCMs with parameterized convection have been shown in several studies to be significantly reduced when using CPMs (Prein et al. 2013; Ban et al. 2014).

Here, we sample a set of summer seasons over Europe and the Alps using different setups with a new regional climate model, the HIRLAM–ALADIN Regional Mesoscale Operational NWP in Europe (HARMONIE) Climate (Lindstedt et al. 2015). Three model configurations were applied; two were integrated at 15- and 6.25-km horizontal resolution using a convection scheme particularly designed for resolutions within the gray zone. The third setup employs a physics package designed for convection-permitting resolutions and is run at 2-km resolution. With this suite of simulations, we aim to investigate the quality of each model version in terms of the

spatial and temporal characteristics of summer precipitation in the Alpine region on daily and subdaily time scales. Specifically, does the 2-km model behave differently concerning precipitation extremes and capture intensities, durations, and frequencies of precipitation spells better than the coarser models using a convective parameterization? Also, do we benefit from using HARMONIE at 6.25-km resolution compared to 15 km (i.e., is there added value already at this intermediate resolution compared to its coarser version)?

2. Experiment setup

a. Models

HARMONIE is a seamless NWP model framework developed jointly between several European national meteorological services. The model system provides flexibility as it contains a suite of different physics packages, each adapted for different horizontal resolutions. Here we have applied two different model setups using the cy37h1.2 climate model version of HARMONIE (HCLIM): 1) a setup with the ALARO physics [a transitional step between ALADIN and Applications of Research to Operations at Mesoscale (AROME); Gerard 2007; Gerard et al. 2009; Piriou et al. 2007] applying the Modular Multiscale Microphysics and Transport (3MT) (Piriou et al. 2007; Gerard et al. 2009) convection parameterization (CP) scheme, applied at two horizontal resolutions, 15 and 6.25 km (HCLIM15 and HCLIM6, respectively); and 2) a setup with the AROME physics package (Seity et al. 2011). AROME is specifically developed to be run at convection-permitting resolutions resolving deep convection explicitly and is here applied to a resolution of 2 km (HCLIM2).

In HARMONIE, irrespective of physics package, the ALADIN-NH provides the nonhydrostatic dynamical core (Bénard et al. 2010), solving the fully compressible Euler equations using a two time level, semi-implicit, semi-Lagrangian discretization on an Arakawa A grid. Here, HCLIM15 and HCLIM6, with ALARO physics, used the hydrostatic version of the dynamical core. The surface parameterization framework is surface externalisée (SURFEX) (Masson et al. 2013), originating from the Interactions between Soil, Biosphere, and Atmosphere (ISBA) surface scheme (Noilhan and Planton 1989). A more thorough description of SURFEX is found in Le Moigne et al. (2012).

Differences between ALARO and AROME appear primarily in the atmospheric physics. In ALARO, radiation is parameterized using the two-stream scheme developed by Ritter and Geleyn (1992) with optical

cloud properties following Mašek (2005). Deep convection in ALARO is not explicitly resolved and uses the 3MT parameterization scheme. In standard parameterizations, separate schemes are used for deep convection and for “nonconvective” (i.e., resolved large scale) clouds, with microphysical conversion to precipitation treated separately in each scheme. However, at ever-higher resolution, the risk of double counting convective processes (both through resolved and parameterized parts) increases, and 3MT handles this by formally separating the two different contributions (Lindstedt et al. 2015). The microphysical processes handle five prognostic water phases, where autoconversion and evaporation are computed level by level (Gerard et al. 2009). The turbulence parameterization is a pseudoprognostic turbulent kinetic energy (pTKE) scheme, which is an extension of the Louis-type vertical diffusion scheme (Louis 1979).

AROME parameterizes radiation using a two-stream approximation in model columns and the effects of surface slopes accounted for. Shortwave and longwave spectral computations follow Fouquart and Bonnel (1980) and Mlawer et al. (1997), respectively, and cloud optical properties for liquid clouds are derived from Morcrette and Fouquart (1986) and from Ebert and Curry (1992) for ice clouds. AROME uses a mixed-phase microphysics scheme, the ICE3 scheme (Pinty and Jabouille 1998), wherein cloud water and ice as well as rain, snow, and graupel are prognostic variables. Hail is assumed to behave as large graupel particles. The turbulence parameterization was developed by Cuxart et al. (2000) and is based on a prognostic TKE equation combined with a diagnostic mixing length L .

A suite of seven summers have been simulated: 1998, 2000, 2002, 2004, 2006, 2007, and 2010. All simulations were initialized in May of each year and run until the end of August, with May omitted from subsequent analysis. HCLIM15 and HCLIM6 were applied over a domain covering Europe (300×320 and 720×800 grid boxes, respectively). Lateral boundary conditions are provided by ERA-Interim (Dee et al. 2011) every 6 h. HCLIM15 was then downscaled by HCLIM2 over a domain covering the Alpine region (see Fig. 1), consisting of 480×360 grid boxes. In this downscaling the lateral boundaries were provided by HCLIM15 every 3 h. All HCLIM simulations have 65 levels in the vertical.

b. Area of investigation

The black rectangle in the left panel in Fig. 1 depicts the investigated area in this study, which covers the nested domain of HCLIM2. For analysis of subdaily precipitation, only Switzerland was considered (Fig. 1,

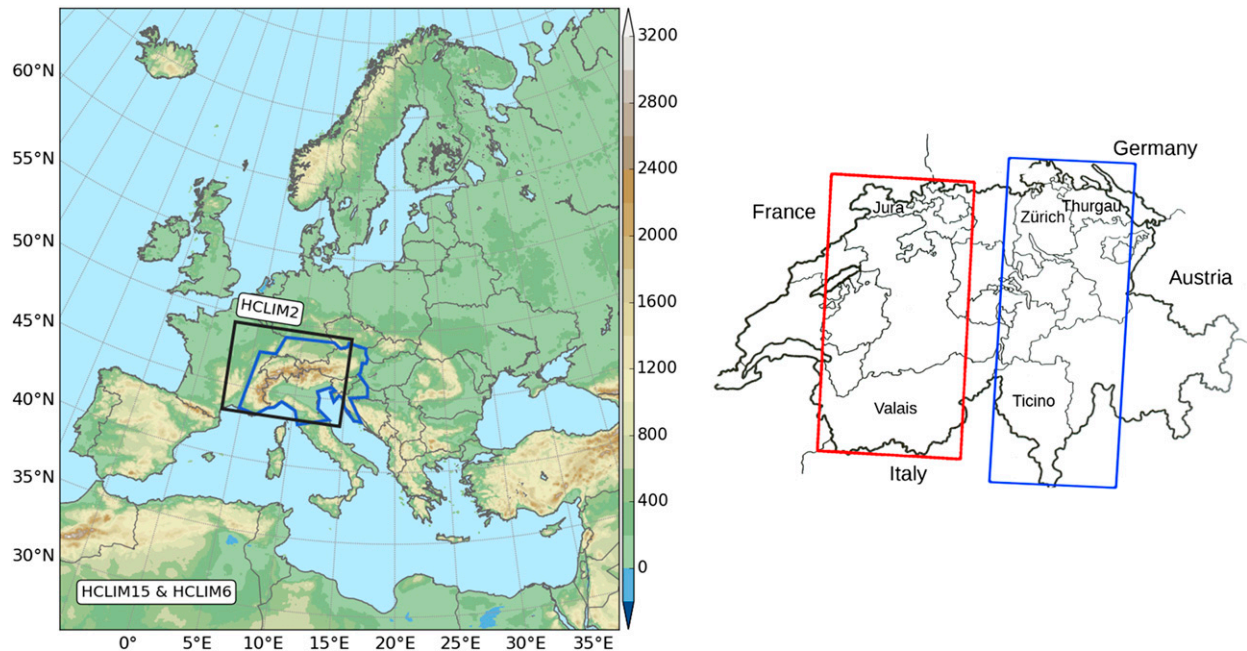


FIG. 1. (left) The domains used for the dynamical downscaling of HCLIM. The pan-Europe outer domain is used for HCLIM15 and HCLIM6, while the inner domain marked by the black box is used for HCLIM2. The blue polygon depicts the domain of the EURO4M observational dataset. Color scale represents model orography (m) originating from HCLIM6. (right) Map of Switzerland. The rectangles depict the western (red) and eastern (blue) segments used in section 4a. (Zonal means are calculated before they are plotted in Fig. 4.)

right panel), as suitable observations were only available for this area. Within the HCLIM2 domain, the most prominent characteristic is the arc-shaped mountain range of the European Alps with an average height of approximately 2500 m, a length of 800 km, and a width ranging from about 100 to 300 km. The ridge is intersected by a series of deep valleys, dividing the range into major mountain massifs. The mountain range has a significant influence on the large-scale atmospheric flow and on the generation of local to mesoscale circulation patterns, acting as a triggering mechanism for convection. With this topographical diversity, as well as its proximity to several large-scale climate regimes (e.g., Mediterranean and European continental climates), this area is both meteorologically interesting and a challenge to simulate correctly.

c. Evaluation data

To account for the large spatial and temporal variability in precipitation, it is often necessary to include multiple observations in model evaluation. In this study we use a number of observational datasets that fulfill the conditions of having sufficient spatial coverage and high-enough temporal resolution to investigate the statistical behavior of convective precipitation in HCLIM on hourly to daily time scales.

European Reanalysis and Observations for Monitoring project (EURO4M) Alpine precipitation grid dataset (APGD) (EURO4M-APGD, hereafter EURO4M; Isotta et al. 2014) is a gridded dataset covering the Alps and adjacent forelands. It consists of rain gauge data from an average of 5500 daily measurements, covering the time period 1971–2008. A distance–angular weighting method was used to interpolate point measurements to daily time scale on a 5-km regular grid. Scales that are effectively resolved are coarser, depend on station density, and vary both in time and space. Interstation spacing sets an approximate lower limit of the effective resolution for daily totals, and in high-density areas this is around 10–15 km (Isotta et al. 2014). The smoothing effect from the interpolation and the inherent uncertainties in gauge measurements affect the quality of the end product. Although gauge undercatch is most prominent in winter (Adam and Lettenmeier 2003), the localized and intermittent nature of convective precipitation in summer causes systematic biases in the observations (Isotta et al. 2014; Rubel and Hantel 2001). Generally, in EURO4M, high intensities are underestimated and low intensities overestimated (Isotta et al. 2014).

To investigate hourly precipitation the RdisaggH dataset is used (Wüest et al. 2010). Combining weather

radar and daily precipitation totals, it consists of hourly precipitation estimates on a 1-km mesh grid over Switzerland for the years 2004–10. The method involves disaggregating rain gauge data using radar, and, therefore, the advantage of the high temporal resolution of radar can be utilized while reducing the impact of its quantitative biases. Validation, through a systematic comparison of RdisaggH at the location of 72 rain gauge stations in Switzerland, shows that errors in intensity and frequency are smaller than 25%, with larger errors in regions with deep valleys due to shielding of the radar beam (Wüest et al. 2010).

3. Methodology

To assess the realism of the simulated precipitation distribution and spell duration, a number of statistical methods have been adopted. Generally, statistical analysis of daily and subdaily precipitation, whereby a significant part may or may not consist of zero values (i.e., dry days, hours, etc.), commonly involves thresholding the data. This subselection of data can have a significant impact on the resulting analysis (changing sample sizes) and therefore should be considered carefully. HCLIM demonstrates a clear underestimation of dry days and hours in the Alpine region. Compared to EURO4M (RdisaggH) HCLIM2, HCLIM6, and HCLIM15 underestimate the fraction of dry days (hours) by 35%, 19%, and 23% (20%, 29%, and 41%) over the Alpine region (Switzerland), respectively. The too-frequent wet hours and days are spatially mostly associated with the steep topography of the Alps. This indicates that HCLIM, both with and without convection parameterization, too easily triggers precipitation-producing processes in interaction with this strong surface forcing. However, a definite explanation for this deficiency demands a more in-depth analysis that is beyond the scope of this study. Keeping in mind these biases, the statistical methods used in this study will mainly focus on when it actually rains, hence using, unless otherwise stated, thresholds to extract wet days or hours. We employ thresholds of 1 mm day^{-1} and 0.1 mm h^{-1} for definition of wet events.

a. Fractions skill score

Roberts and Lean (2008) introduced a method, called fractions skill score (FSS), that fits into the neighborhood verification category. This will be a short overview of the method, and for a detailed description the reader is referred to Roberts and Lean (2008). The main purpose of FSS is to provide an objective way to assess how the skill in high-resolution numerical models varies with spatial scale. FSS gives information on realism in terms

of spatial frequency and, furthermore, the smallest spatial scale where the simulations can be considered skillful. The computation of FSS is performed in a two-step operation: First, a threshold is applied to grid points of model data and observations, converting them into binary fields (1 above threshold, 0 otherwise). Second, the fraction of pixels exceeding the threshold within a specified neighborhood of each grid point is then compared between model and observations. This set of operations is repeated for a number of thresholds and neighborhoods, ranging in sizes from a single pixel to the entire domain. Values of FSS can range from 0, corresponding to no skill, to 1, perfect skill. FSS typically increases from a minimum value for gridpoint scales to larger values as the neighborhood area gets larger, asymptotically reaching its maximum value for large neighborhoods. The maximum value would be 1 if no bias were present in the model; otherwise it asymptotes to a lower value. Roberts and Lean (2008) defined a smallest neighborhood size for which a sufficient skill is achieved—when $FSS_u = 0.5 + f_o/2$ is obtained, where f_o is the observed wet area fraction in the domain. The skill of a random forecast that has the same fractional coverage of precipitation over the whole domain as observations is given by $FSS_r = f_o$ and sets a minimum level of skill. The FSS calculation is performed for every time step chosen (e.g., hourly). Prior to this, both observations and model data must be interpolated to the same grid configuration. Here, we aggregate all data on to the coarsest 15-km grid, and the domain is limited to the RdisaggH coverage (i.e., the area of Switzerland).

b. Event duration analysis

A more complete analysis would encompass a temporal aspect as well. Therefore, we include an analysis to address the realism of the simulated precipitation in terms of the duration of precipitation spells, mainly following the methodology of Kendon et al. (2012). All grid points covered by both models and RdisaggH observations, the area of Switzerland, are considered. We use all seven summers of model data and all RdisaggH data, even though there is not a complete overlap between these. A sensitivity test by using only overlapping data did not alter the results significantly, and we chose to use as much data as possible to increase the statistical robustness. All data are aggregated to the HCLIM15 grid prior to analysis.

For each grid pixel, events are identified as occurrences of precipitation above a certain threshold. The duration of an event consists of the number of coherent hours of precipitation above the threshold. During a spell, the intensity of precipitation varies, and it varies differently depending on the nature of the process,

comparing for example a localized convective rainfall event and a warm frontal passage. To assess this, we record the peak intensity of each identified event. Further on, percentile thresholds are used in the analysis, thereby avoiding the effect of possible biases in model data. In particular, to focus on the upper tail of the precipitation distributions, a number of high percentiles are used and are calculated for all grid points and all hours (wet plus dry) within the domain for models and observations separately. The statistics assembled through this methodology provide the basis for the computation of probability distributions of spell duration and intensity.

The significance of model–observation differences are assessed using a block bootstrap method (Efron and Tibshirani 1993). Autocorrelation of the data is considered by the use of blocks, and here the block size is set to the number of hours per summer season. For each pixel 500 resamplings are generated, and all these surrogate time series undergo the same statistical analysis as described above, resulting in 500 probability distributions for duration and peak intensities. From this we can calculate 500 differences between model and observations (or between different model versions). If the 99% confidence interval of these differences does not include zero, the difference is considered statistically significant at the 1% level.

c. Statistical analysis of hourly extremes

By the very nature of extremes, the rarity of events makes the robustness of a direct analysis of them weak, and one needs to apply statistical methods and models specifically designed for the tail behavior of distributions. In this study we employ the peak-over-threshold (PoT) method, which exclusively describes the characteristics of precipitation events that exceeds a high-enough threshold (Coles 2001). PoT has recently been applied in several studies of extreme precipitation at daily and subdaily time scales (e.g., Fröh et al. 2010; Feldmann et al. 2013; Chan et al. 2014). The well-known asymptotic three-parameter generalized Pareto distribution (GPD) (Hosking and Wallis 1987) is used to describe the behavior of the PoT events, and the associated parameter estimation is performed using the method of L moments (Hosking 1990). The latter is the preferred method of estimation for small data samples, as is the case here, over other methods like maximum likelihood (Hosking and Wallis 1987). GPDs are defined by α , k , and ξ , which represent the scale (describing the dispersion), the shape (analogous to skewness), and the location (equivalent to the threshold for exceedances), respectively. The cumulative distribution function is then given by the following:

$$F_{(k,\xi,\alpha)}(x) = \begin{cases} 1 - \left[1 + \frac{k(x - \xi)}{\alpha} \right]^{-1/k}, & k \neq 0 \\ 1 - \exp \left[-\frac{(x - \xi)}{\alpha} \right], & k = 0 \end{cases}. \quad (1)$$

Use of PoT entails the sampling of data that exceed a predefined threshold, a limit that should be high enough to ensure that the assumptions of the statistical model are justified and low enough to capture a reasonable number of events. Recent literature suggest the use of a (wet) percentile threshold in the range of 90%–95% (e.g., Chan et al. 2014; Feldmann et al. 2013; Tomassini and Jacob 2009), and we deploy in this study the 95th percentile of wet values (>0.1 mm). The underlying precipitation data are highly susceptible to serial correlation, and to make sure that only distinct events are used, we apply an automatic declustering technique developed by Ferro and Segers (2003). Also, to increase robustness, the PoT analysis is applied to pooled grid points; the nearest neighbors of each grid point (i.e., a total of nine grid points) are included in all separate calculations. We do this under the assumption that the threshold of the actual grid point is valid for all of the pooled members. However, in areas with very strong spatial gradients in precipitation (climatologically) this assumption may not be completely valid.

4. Results and discussion

a. Spatial distribution and frequency analysis

Figures 2 and 3 present the spatial distribution of daily and hourly precipitation statistics over the Alps and Switzerland, respectively. Although HCLIM is generally able to represent the overall spatial distribution of summer mean daily precipitation, including the complex variability within the Alps massifs, it clearly overestimates precipitation in mountainous areas, especially in HCLIM2, which has a strong correlation between wet biases and topographic features. A summer wet bias in the Alps compared to EURO4M has been seen in other RCMs and CPCMs (e.g., Ban et al. 2014), although not as large as in HCLIM. The wet biases over the Alpine peaks and crests are mostly due to too-frequent precipitation events as clearly seen for hourly precipitation statistics over Switzerland (Fig. 3, top) comparing models to RdisaggH observations. It is most notable in HCLIM6 and HCLIM15, while, interestingly, they concurrently underestimate the mean wet hour intensity (Fig. 3, middle). In the southern Alpine regions fewer wet hours are observed, which is relatively well simulated by HCLIM2, but in HCLIM6 and HCLIM15 this is highly overestimated apart from southern Ticino.

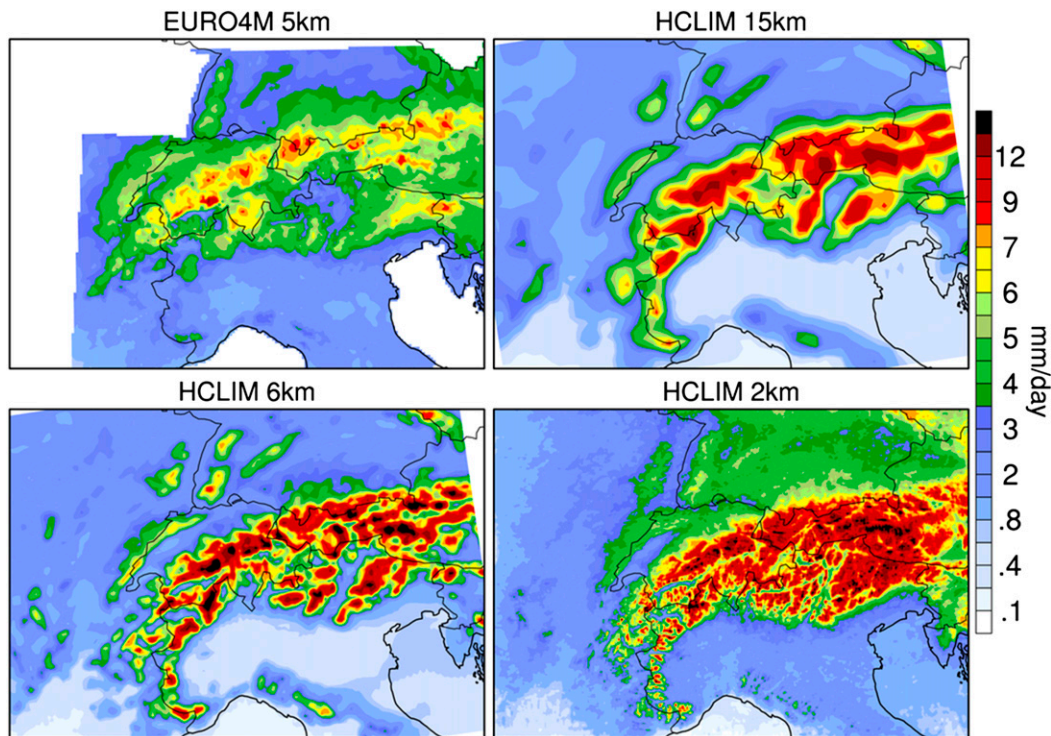


FIG. 2. The summer [June–August (JJA)] season mean daily precipitation from the HCLIM simulations and EURO4M. All data are on their original resolution grids.

Interestingly, the observed mean intensity of wet hours has a distinct maximum in the Ticino area; thus this area is exposed to few but quite vigorous rain spell events (Isotta et al. 2014). This is also supported by considering the fraction of total precipitation received from intensities in the upper part of the distribution (Fig. 3, bottom). This combined characteristic is much better simulated in HCLIM2 compared to the other HCLIM versions. In the northernmost part, on the other hand, HCLIM2 underestimates the frequency but overestimates the intensity of events, while in HCLIM6 and HCLIM15 it is the other way around. Note that in the southeastern and to some extent in the southwestern part of Switzerland, the quality of RdisaggH observations is relatively low, primarily because of low radar data coverage and radar beam shielding effects due to steep topography (Wüest et al. 2010), and the interpretation of results in these areas should be done with caution.

One major benefit of increased model resolution is expected to occur in mountainous regions as the finer-mesh grid provides a more detailed representation of orography and hence of surface forcing. In Fig. 4 this expected behavior is further explored. The rate of precipitation as a function of altitude (Fig. 4, top) in observations and HCLIM shows that RdisaggH and

HCLIM2 exhibit qualitatively similar behavior for daily amounts with an increase in rates up to around 1000 m. However, there is a clear underestimation of HCLIM6 and HCLIM15 for these lower-lying areas (see also Fig. 2). Above this altitude, the patterns diverge; in all versions of HCLIM the rates continue to increase until about 2000 m, while EURO4M reaches a maximum just below about 1500 m and then starts to decrease. It is worth mentioning that at the higher elevations, EURO4M most likely underestimates precipitation amounts because of a lack of observations (Isotta et al. 2014). Although HCLIM2 has distinctly larger absolute values, it does capture the overall decrease at higher altitudes in closer agreement with EURO4M than the coarser simulations. Over Switzerland, for the hourly precipitation rates, the dependence on altitude is also remarkably similar between RdisaggH and HCLIM2. Differences between HCLIM6 and HCLIM15 are generally small.

The observed trans-Alpine character of hourly averages (Fig. 4, bottom) exhibits a shielding effect in both the eastern and western parts, manifest as minimum values at or close to shallow valleys within the Alpine crest areas. This is well captured by the models. On the northern slopes there is an observed increase in precipitation rate followed by decreases in the flat areas

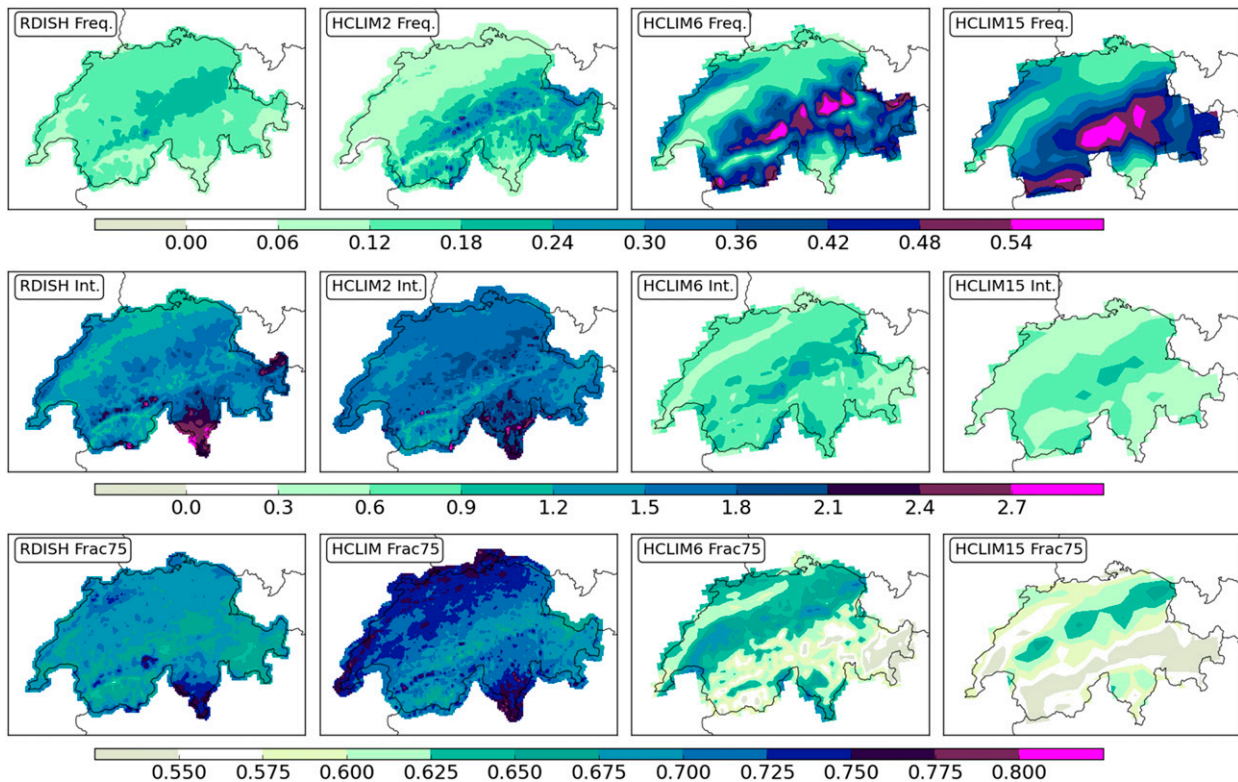


FIG. 3. Precipitation statistics over Switzerland. (left)–(right) RdisaggH, HCLIM2, HCLIM6, and HCLIM15 using the following statistics: (top) wet hour frequency (fraction), (middle) mean wet hour intensity (mm h^{-1}), and (bottom) fraction of precipitation from hours with moderate-to-high intensity (≥ 75 th percentile on wet hours; fraction). All data are kept at their respective horizontal resolutions.

farther north, a pattern that is broadly seen also in HCLIM; however, HCLIM2 shows greater realism than HCLIM6. Note the strong increase in precipitation from the crest and southward, an area frequently subjected to heavy precipitation events in the mesoscale during summer and fall (Isotta et al. 2014; Frei and Schär 1998), again well captured by HCLIM2 but weak and erratic in HCLIM6.

Frequency–intensity distributions of daily and hourly precipitation totals are presented in Fig. 5. Only wet days and hours are considered in the analysis. On daily time scales, HCLIM shows good agreement with EURO4M. HCLIM2 overestimates the moderate-to-strong events ($\sim 20\text{--}40\text{ mm day}^{-1}$), while HCLIM6 and HCLIM15 underestimate these. For the very extreme events, there is a good resemblance between HCLIM and EURO4M, most clearly seen in the inset figure, showing only the highest intensities, with models and observations on their native grid. Here, HCLIM6 shows an exceptionally close agreement with EURO4M, as does HCLIM2 but not to the same extent, while HCLIM15 systematically underestimates the probabilities. For the hourly estimates, the results are markedly different. The resolution and explicit or nonexplicit convection dependencies

become evident. With outstanding accuracy, HCLIM2 matches RdisaggH over almost the complete spectrum of intensities, whereas HCLIM6 and HCLIM15 already have statistically significant (as depicted by the 95% confidence interval) lower probabilities for moderate intensities and then continuously lower probabilities for successively stronger intensities. HCLIM6 does, however, perform somewhat better than HCLIM15, which signifies some added value from the increased model resolution.

The results so far confirm the commonly stated conclusion from multiple other studies that RCMs at meso- γ horizontal resolution with convection parameterization schemes may be able to reproduce observed frequency–intensity distributions of daily accumulated precipitation; however, on the subdaily time scales, they are generally outperformed by CPCMs (e.g., Ban et al. 2014; Fosser et al. 2015). Precipitation extremes and associated high-impact events such as flash floods most often involve convective processes with life time spans of a few hours (Ulbrich et al. 2003; Doswell et al. 1996). This highlights the importance of the subdaily time evolution of precipitation, especially during summer with rainfall of predominantly convective origin, and

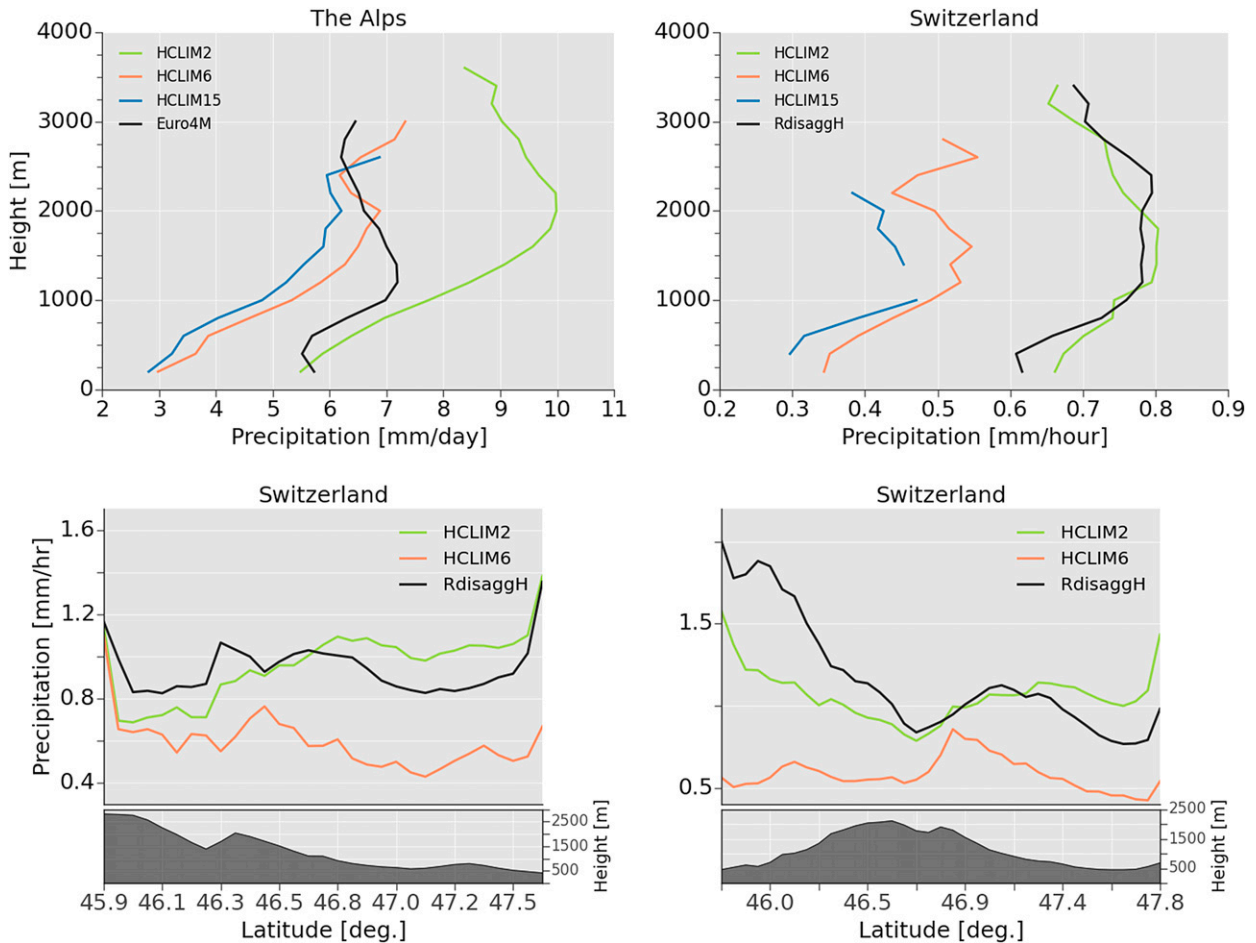


FIG. 4. Precipitation rate dependency on height. (top) Precipitation rates have been binned into 200-m height intervals, and in each bin the median value is computed. At least 10 grid points need to exist in each bin. No prior horizontal aggregation has been performed for any of the data. (bottom) North–south cross sections of hourly gridpoint-average precipitation over (left) western and (right) eastern Switzerland (see Fig. 1 for the definition of the segments). In the bottom panels the orography from HCLIM6 is shown, and here all data have been interpolated onto the 6-km grid.

how it is represented in climate models (Kendon et al. 2012). It is important to note that there is generally better agreement between HCLIM2 and RdisaggH on hourly time scales than on daily time scales (where RdisaggH is in agreement with EURO4M; not shown), suggesting that analysis is sensitive to thresholding of data. In addition, small hourly biases accumulate to larger (relative) values when aggregated to daily intensities (Fig. 3).

b. Extremes

How are hourly precipitation extremes represented in HCLIM? Because of the inherent uncertainty associated with extremes (very low frequency) and the relatively short-term simulations in this study, we address this question by extending the basic validation (Figs. 3 and 5) with extreme value analysis, adopting the PoT statistical model (section 3c). This provides a much more

complete analysis of the statistical distribution of extreme rainfall events.

The parameters that define the extreme value distributions over Switzerland in HCLIM and RdisaggH are shown in Fig. 6. For brevity only HCLIM2 and HCLIM6 are included in the figure, showing analysis made on the 6-km grid resolution. An analysis performed on the 15-km grid showed that HCLIM15, at best, showed similar but mostly less accurate results than HCLIM6. The scale α and shape k parameters are diagnostics of the dispersion (analog to standard deviation) and skewness (thinness/thickness of the tail) of the distribution, respectively (section 3c). The spatially averaged scale parameter is somewhat overestimated in HCLIM2, mostly resulting from the larger estimates in northern Switzerland, but otherwise is in good agreement. Conversely, HCLIM6 has too “narrow” extreme value

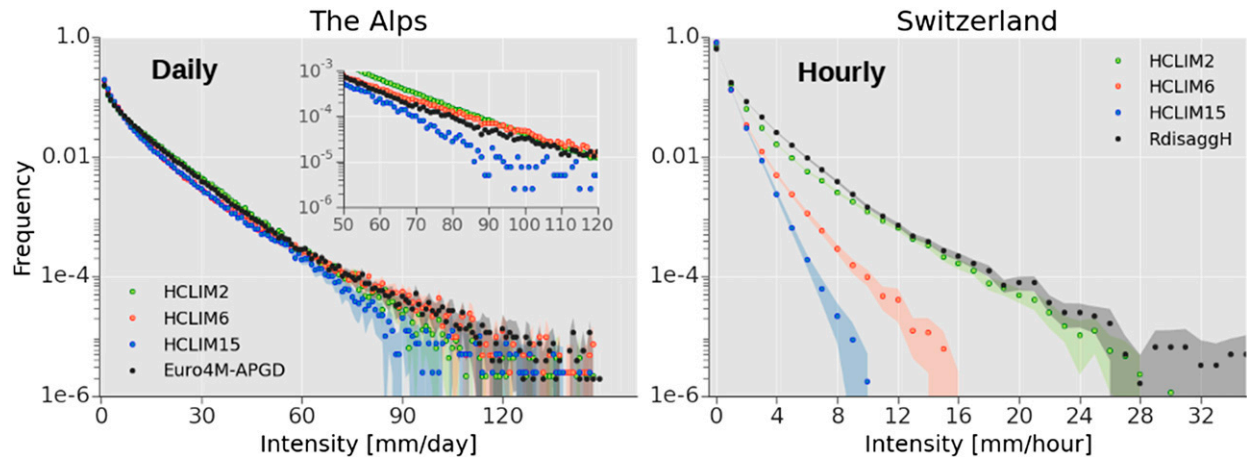


FIG. 5. Empirical probability distribution functions of (left) daily and (right) hourly accumulated precipitation rates. All data have been interpolated to the 15-km grid, except in the inset plot where data are kept at their native grid resolution. The shading represents the 95% confidence interval computed from a bootstrap calculation using 500 resamples. The Alps area is defined by the area of EURO4M (see Fig. 1).

distributions reflected in the lower estimates in most parts of the domain. The highest values are observed in Ticino, which is consistent with the few but vigorous events seen in this area (Fig. 3). HCLIM2 is able to reproduce this maximum but this is much lower in HCLIM6 (barely perceptible in HCLIM15; not shown). HCLIM has trouble reproducing the skewness; HCLIM2 has overall a somewhat thin tail and HCLIM6 has better spatial mean but larger regional differences. Interestingly, HCLIM2 (HCLIM6) underestimates (overestimates) the skewness in Ticino. The threshold for exceedances (location, defined here by the 95th percentile of wet hours) is well captured by HCLIM2, with a similar spatial average as in RdisaggH but for example too high estimates in the north. In HCLIM6 the location is clearly underestimated throughout the domain.

These parameters form the basis from which one may extrapolate the behavior of extreme precipitation beyond the considered time scale. Return levels z , defined as the (high) quantile value of the GPD distribution, which is exceeded, on average, once every T years, the return period. Using the quantile function, which is the inverse of Eq. (1), and the estimated crossing rate λ (i.e., the expected number of events exceeding the threshold per year or season), the return level is given by the following:

$$z(T | \xi, \alpha, k) = \begin{cases} \xi + \frac{\alpha}{k} [(\lambda T)^k - 1], & k \neq 0 \\ \xi + \alpha \ln(\lambda T), & k = 0 \end{cases}, \quad (2)$$

where ξ , α , and k are the GPD parameters. Estimates of z as a function of $\log_{10}(T)$ are shown in Fig. 7, the lines representing the domain average values. We again only

consider HCLIM2 and HCLIM6 because HCLIM15 severely underestimates all return levels (not shown). In addition to hourly return levels, the data have been aggregated in time to 6 and 12 h, respectively, to investigate the sensitivity to the temporal evolution of events (in a statistical sense). As only seven seasons have been sampled, the uncertainty for return levels of large T is large. In Fig. 7 return levels for $T > 20$ years have therefore been shaded in dark gray to emphasize this uncertainty. For all accumulations HCLIM underestimates the return levels for the full range of recurrence intervals T —however, with clear differences between HCLIM2 and HCLIM6. At hourly accumulations, the former is rather close to RdisaggH, especially for shorter return periods. Conversely, HCLIM6 significantly underestimates the return levels across all return periods, which is due to the clearly too-low values of the threshold ξ and scale α parameters (Fig. 6). Despite this, in both model and observations there is a similar quasi-linear increase of z with $\log(T)$, reflecting the near-zero values of the shape parameter k (Fig. 6). HCLIM2 has a lower mean value than HCLIM6 and RdisaggH and thus also has the smallest rate of increase of z with $\log(T)$. The slight underestimation in both HCLIM2 and HCLIM6 in this rate of increase compared to observations leads to negative biases becoming larger for larger T .

Similar behavior is seen for the 6-h accumulations (and also for 3-h accumulations, although here HCLIM2 match RdisaggH almost perfectly for all T ; not shown), which indicates an insensitivity to accumulation periods of a few hours. However, there is a sharp shift in the results for 12-h accumulations. Both model versions significantly underestimate the return levels and their

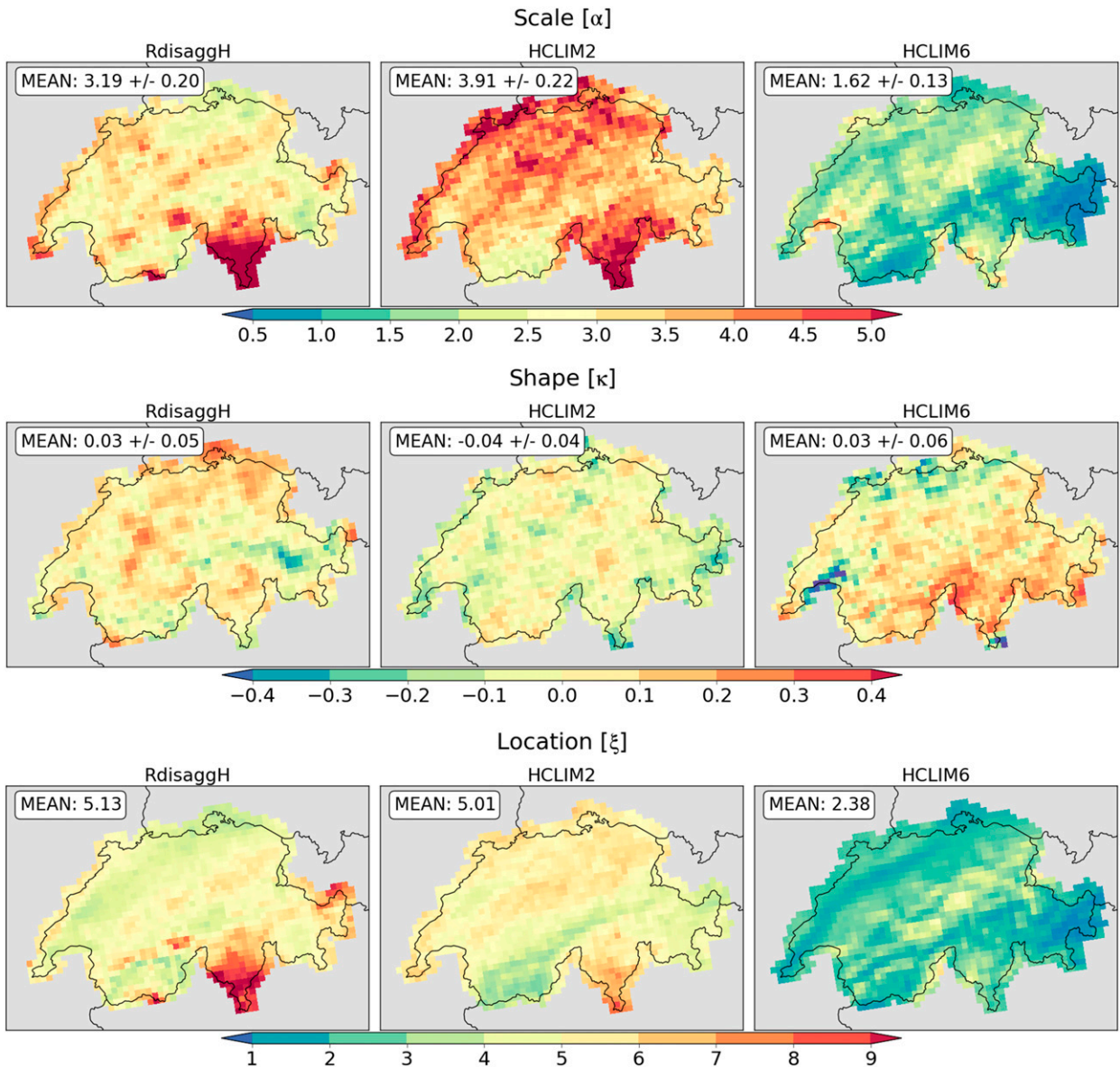


FIG. 6. PoT-fitted parameters: (top) scale (mm h^{-1}), (middle) shape (dimensionless), and (bottom) location (mm h^{-1}) in (left) RdisaggH, (center) HCLIM2, and (right) HCLIM6. See text for more details.

rate of increase. A closer examination reveals that the differences in z are mainly attributed to much higher values in RdisaggH in the western part of Switzerland, an area with relatively low frequency of rain spells, which on average are moderate or weak (Fig. 3). Hence, the nonextreme nature of precipitation in this area may not be adequately described by the GP distribution. Chan et al. (2014) performed a similar extreme value analysis for the southern United Kingdom using a regional climate model at 12- and 1.5-km resolution, the latter treating deep convection explicitly. In accordance with our results, the high-resolution model outperformed the

RCM with CP and coarser grid in the summer season. Even though the convection-permitting model tended to overestimate return levels, the coarser model had difficulties representing the rate of increase of z with T because of an overestimated shape parameter. Here, HCLIM6 is actually able to realistically represent this statistical behavior but struggles with the intensity of extremes, thereby reducing the realism.

c. Spatial frequency of precipitation

Figure 8 depicts two-dimensional representations of FSS over Switzerland, with threshold along the ordinate

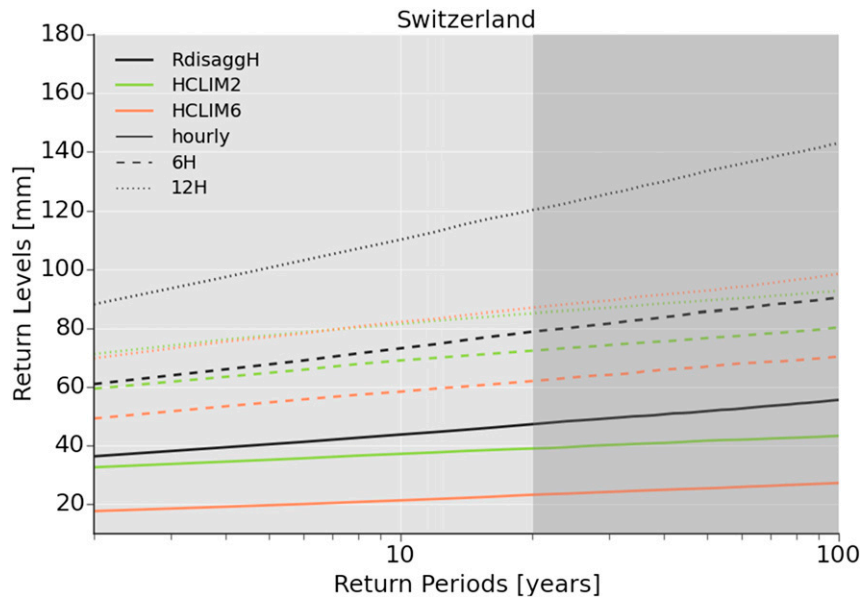


FIG. 7. Calculated return levels [Eq. (2)] as a function of return periods from the PoT analysis. See text for more details.

and the horizontal scale on the abscissa. The typical behavior, seen in the leftmost panel, is that FSS values increase for larger horizontal scales and decrease for higher thresholds. We choose to show results for 3-hourly accumulations to increase the signal for the higher thresholds; however, the main results do not change for other accumulation times. It is evident from the figure that at higher intensities, HCLIM2 has larger FSS values (more reddish color on the right-hand sides), signifying better spatial frequency of high-intensity events in HCLIM2 compared to HCLIM6 and HCLIM15. It should be noted that for the highest thresholds, the signal is weak (i.e., few events), which undermines the robustness of the results. Furthermore, there is no clear difference between HCLIM6 and HCLIM15, at least on these spatial scales. Figure 9 presents FSS as a function of horizontal scale for a few selected thresholds—namely, 0.5, 2, and 5 mm h⁻¹ and 15 mm (3 h)⁻¹, respectively. Already at the lowest threshold, HCLIM2 generates higher FSS than the coarser simulations, and differences become increasingly evident the higher the intensity threshold (although the significance of the differences is, as mentioned, low for the higher-intensity thresholds). For 2 and 5 mm h⁻¹ intensity limits, HCLIM2 reaches random skill faster than HCLIM6 and HCLIM15, at approximately 15–30-km smaller horizontal scales, and the upper skill is passed at approximately 30–60-km shorter scales. For the highest rate, upper skill is achieved at around 200 km in HCLIM2, almost 150 km earlier than HCLIM6, not

being reached at all in HCLIM15. Similar results have been achieved elsewhere; for example, in a suite of CPCM and RCM simulations at 3–10-km resolutions over the Alps region, Prein et al. (2013) showed that the CPCMs performed better with higher FSS values and skills reached for much smaller spatial scales than the coarser RCMs.

It is worth reemphasizing that the FSS analysis does not directly diagnose particular physical aspects of the simulated precipitation processes such as areal extent or intensity. However, another important property of precipitation is the frequency of exceeding a critical threshold, which can be interpreted as the probability for a severe event, and in this respect FSS provides valuable information. Furthermore, we have used absolute threshold values in the analysis, and therefore, positive results tend to bias toward higher-resolution models for higher thresholds as they in general have larger probabilities for occurrences of such events (assuming no severe deficiencies in the model physics such as the convection parameterization). Nonetheless, the purpose of this study is to examine and quantify the added value using a CPM version of HCLIM compared to the version with parameterized convection, especially in terms of realism. Therefore, we find it preferable in the FSS analysis to use absolute thresholds instead of relative (percentile) thresholds. The results show that HCLIM2 surpasses both skill limits faster than HCLIM6 and HCLIM15, most evidently for stronger-intensity thresholds; hence, there are strong

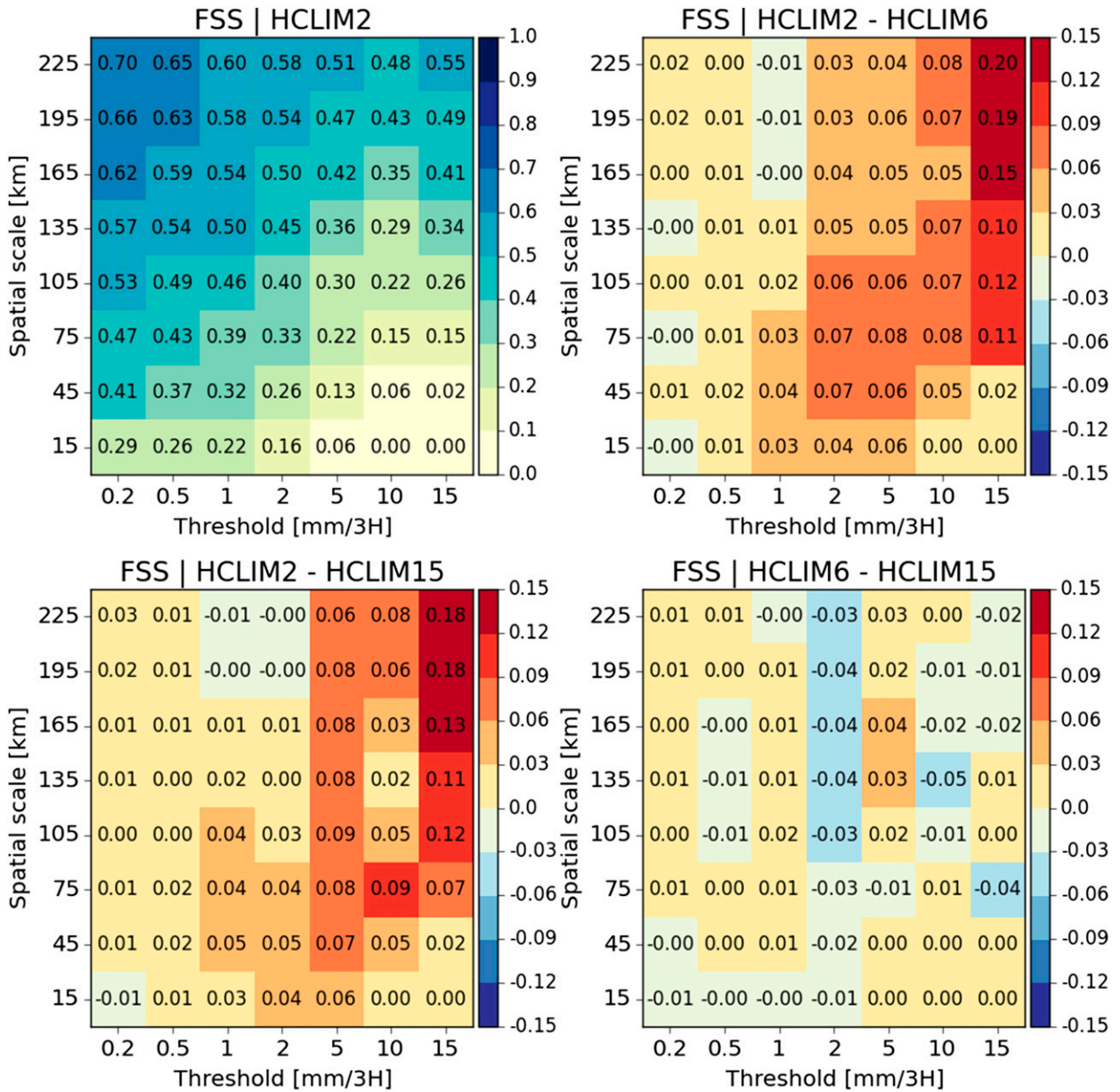


FIG. 8. FSS (colors and values) as a function of neighborhood size (spatial scale) and threshold [mm (3h)⁻¹], computed over the domain of Switzerland using RdisaggH as observations. (top left) HCLIM2 and differences between (top right) HCLIM2 and HCLIM6, (bottom left) HCLIM2 and HCLIM15, and (bottom right) HCLIM6 and HCLIM15.

indications of a higher realism of the spatial frequency of heavy rainfall events in HCLIM2.

d. Spell duration analysis

Apart from accurate spatial distributions (e.g., where it rains), the temporal aspect of precipitation events is also important, as the duration has large impact on the total amount of accumulated precipitation at a specific location. In this last section we explore the duration of precipitation events over Switzerland in RdisaggH and

to what extent HCLIM can reproduce this temporal characteristic. For this, an Eulerian framework is adopted, whereby the duration of events is calculated for each grid point separately. Figure 10 presents the probabilities of rain spell durations for different percentile thresholds used to define the start (and end) of an event. Each row represents a probability distribution of spell durations (*x* axis) for a given threshold (*y* axis). The leftmost panels in Fig. 10 shows the observed probabilities for different percentile thresholds (Fig. 10, top) and peak intensities

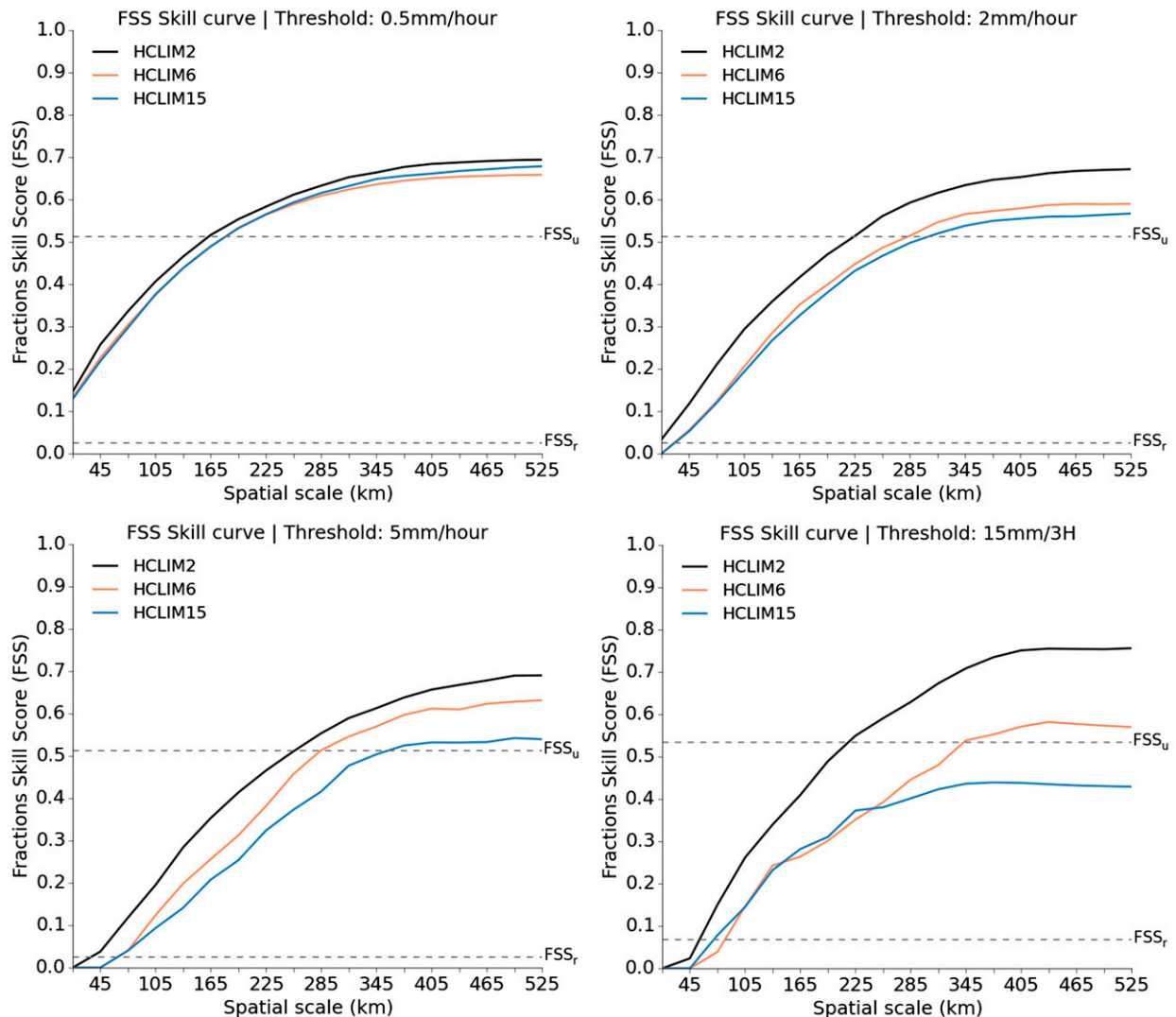


FIG. 9. FSS skill curves computed over Switzerland using RdisaggH observations and for a number of different precipitation intensity thresholds. The colored lines show the medians of FSS. See text for definition and interpretation of FSS_r and FSS_u.

(Fig. 10, bottom). Typically, for the highest percentile thresholds, the duration of rainfall tends to be short, probabilities decreasing quickly for durations of more than a couple of hours. Intuitively, and what is also observed, for lower thresholds there is an increase in the probabilities for events to last longer (e.g., a larger chance of neighboring time steps being included in a single rain event). The observed dependency of peak intensity of the complete rain spells (i.e., using a very low threshold of 0.1 mm h^{-1}) on the duration of events indicates that low peak intensities are usually associated with short-lived events, and moderate-to-strong peak intensities, between approximately 2 and 10 mm h^{-1} , are embedded in spells with a greater range of durations; that is, even for more persistent events (6–12 h), the probabilities remain

relatively high. For the most intense peak values, there are few events (Fig. 5) that are distributed evenly across the event durations. The models have similar behavior, but there are significant differences in the probability distributions as seen in Fig. 10, especially for the coarser HCLIM runs. The latter clearly underestimates the frequency of very short 1–3-hourly events and overestimates the longer-lasting spells. This deficiency is particularly pronounced for the heaviest rain spells (percentiles ≥ 99 th percentile). Furthermore, HCLIM6 and HCLIM15 too frequently produce multihour rain spells with low peak intensities and underestimate the occurrence of short-duration low-to-moderate peak intensity events. These kind of deficiencies have been noted in other RCMs (e.g., Kendon et al. 2012) and is most probably

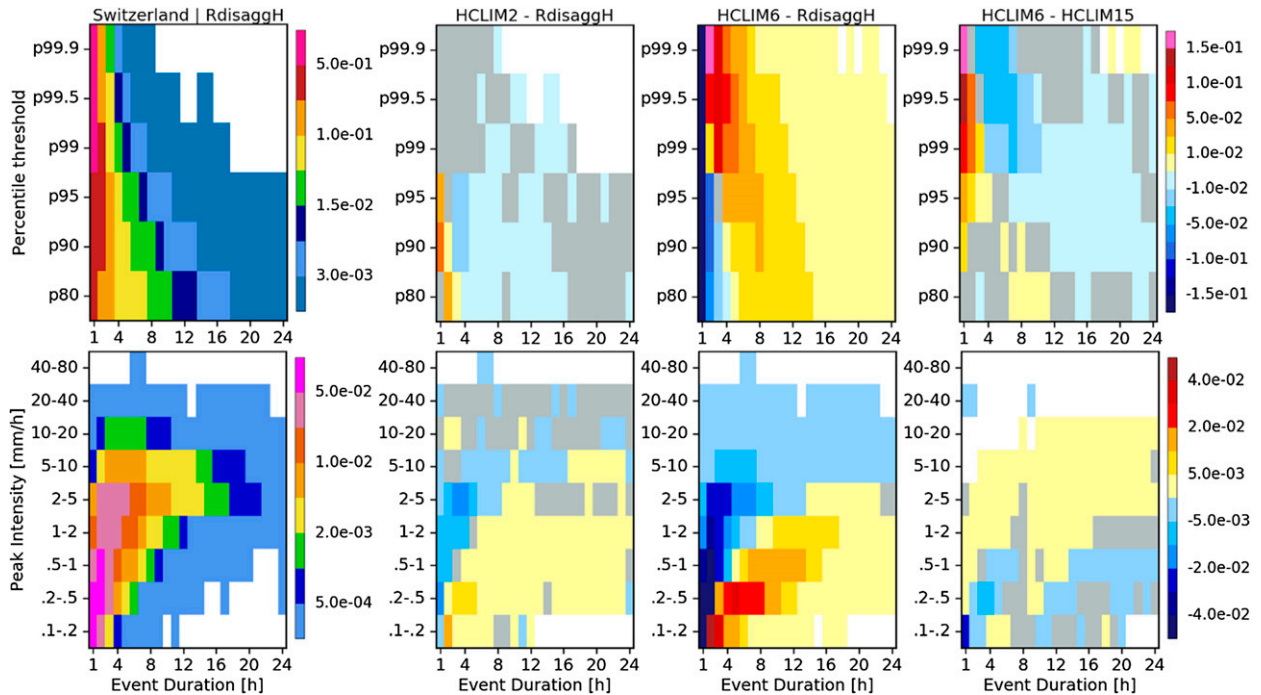


FIG. 10. Probability distributions (top) of spell durations for precipitation exceeding different percentile thresholds and (bottom) for peak intensities given a threshold of 0.1 mm h^{-1} (after Kendon et al. 2012). Differences not statistically significant are shaded in gray, and white means zero probability. Results are shown for (left) RdisaggH, (left center) HCLIM2 minus RdisaggH, (right center) HCLIM6 minus RdisaggH, and (right) HCLIM6 minus HCLIM15.

related (at least in part) to the use of a convective parameterization. This bias pattern is consistent with a problem seen in many climate models; the too early onset of diurnally forced convection, prohibiting the buildup of convective available potential energy and often resulting in a lower late afternoon maximum in convective precipitation rate than observed (e.g., Brockhaus et al. 2008; Kendon et al. 2012; Prein et al. 2013; Ban et al. 2014). For both the duration probabilities and peak intensities, HCLIM6 shows better agreement with observations than HCLIM15 (mostly statistically significant), most clearly for spell durations $\leq 6 \text{ h}$ (Fig. 10, right panels). In stark contrast to these results, HCLIM2 does a much better job at simulating the observed characteristics, signified by the much smaller differences in the probabilities compared to RdisaggH. This largely resembles the results and conclusions of Kendon et al. (2012), although for a different region and model. HCLIM2 does show some overestimation of the occurrence of 1-hourly events for the higher percentiles and slight underestimation for multihourly events, the differences being statistically significant. For the peak intensities, HCLIM2 displays similar behavior to HCLIM6 but with a much reduced bias, and overall there is a

significant improvement in the use of HCLIM2 compared to HCLIM6 and HCLIM15.

5. Conclusions

Accurate model projections of precipitation distribution, especially the frequency and intensity of wet extremes, still remain one of the largest challenges in the climate model community. Commonly, models have errors due to inadequate representation of local and regional forcing and to unresolved processes important for correct storm evolution. Recently, the introduction and application of convection-permitting climate models (CPCMs) at the kilometer-scale resolution has resulted in a marked increase in accuracy and realism of small-scale, convective precipitation events (e.g., Kendon et al. 2012; Prein et al. 2015; Ban et al. 2014) and its extremes (e.g., Chan et al. 2014). However, it still is computationally very expensive to run these models, and the experiments are usually confined to short time periods and/or small domains using a single model. In absence of any large multi-CPCM ensembles to study uncertainties and robustness associated with model differences, introducing new CPCMs in separate experiments and

testing for reproducibility of results adds important information for future applications. Furthermore, the question of cost versus benefit is becoming more and more important to answer within the regional climate modeling community.

In this study we have employed the HCLIM RCM at various resolutions; at 15, 6.25, and 2 km, respectively, over the Alpine region. Seven summers have been sampled and the validation of the intensities, durations, and frequencies of precipitation spells have been studied using high-resolution gridded observations, based on synoptic as well as radar measurements. In contrast to HCLIM2, HCLIM15 and HCLIM6 use a hydrostatic dynamical core and convection parameterization. Our results show HCLIM in general has some problems in the simulation of precipitation distributions. For example, HCLIM underestimates dry days and hours by approximately 20%–40% compared to observations, making the statistical analysis sensitive to thresholding of the data. Also, there is a clear overestimation of precipitation in connection to the Alps crest areas. Despite these issues, we conclude that HCLIM2 is able to represent spatial and temporal (duration) characteristics of subdaily precipitation, including extremes, with a considerable larger realism than its coarser counterparts that uses a convection parameterization scheme. For example, at an intensity of 15 mm (3 h)^{-1} , HCLIM2 attains a predefined level of skill in the simulation of spatial frequency of events at a horizontal scale 36% shorter than HCLIM6, at 220 and 345 km, respectively. The increased realism in HCLIM2 support findings in other similar studies using CPCMs (e.g., Prein et al. 2013; Ban et al. 2014; Kendon et al. 2012; Fosser et al. 2015; Chan et al. 2014) and further points to a distinct advantage of using CPCMs in modeling of subdaily precipitation, particularly in regions where and seasons when deep convection is dominant and also in areas with strong topographical heterogeneity. These are all characteristics that have been shown important in past flash flood events in Europe (e.g., Ulbrich et al. 2003; Lin et al. 2001). With respect to future projections of extreme precipitation using CPCMs, it is worth pointing out that these models, although skillful in representing precipitation processes, are dependent on driving large-scale models to provide good large-scale circulation within which the CPCMs will operate.

With regards to the benefit of “gray zone” resolution, no clear improvement has been shown here in HCLIM6 compared to HCLIM15. HCLIM6 does, however, show larger probabilities for high-intensity events, statistically significantly at hourly time scales, in better agreement with observations. Furthermore, HCLIM6 statistically significantly reduces biases in the duration and peak

intensity of rain spells, particularly for shorter 1–6-h events, and also has a somewhat better skill in the spatial frequency as shown by the FSS analysis. In summary, HCLIM6 shows an improvement compared to HCLIM15—however, not always beyond uncertainties associated with the analysis and not near the improvement seen in HCLIM2. It is worthwhile to consider differences in computational cost. HCLIM6 is about 5 times more expensive as HCLIM15 to run; thus, it may be more reasonable to use a resolution of approximately 10–15 km on the scale of Europe, which is then downscaled by a CPCM, skipping the intermediate resolution. Finally, the use of a CP scheme in RCMs limits the models’ ability to simulate convective events correctly. There are similar issues in this version of HCLIM as well, even though HCLIM uses a scale-independent (down to a few kilometers) scheme. However, no clear conclusions in this matter can really be drawn in this study, and further investigations are needed.

Acknowledgments. Part of this work was done in the IMPACT2C and HELIX projects that receive funding from the European Union Seventh Framework Programme (FP7/2007-2013) under Grant Agreements 282746 and 603864, respectively. The analysis work has also been funded by the Swedish Mistra-SWECIA program funded by Mistra (the Foundation for Strategic Environmental Research) and finally the Hydroimpacts project funded from the Swedish Research Council Formas through Grant 2009-525. The model simulations were performed on the National Supercomputer Centre in Sweden (NSC), which is funded by the Swedish Research Council via Swedish National Infrastructure for Computing (SNIC) and on the ECMWF’s computing facilities. The authors thank MeteoSwiss for providing us with observational datasets (EURO4M-APGD and RdisaggH).

REFERENCES

- Adam, J. C., and D. P. Lettenmeier, 2003: Adjustment of global gridded precipitation for systematic bias. *J. Geophys. Res.*, **108**, 4257, doi:10.1029/2002JD002499.
- Ban, N., J. Schmidli, and C. Schär, 2014: Evaluation of the convection-resolving regional climate modeling approach in decade-long simulations. *J. Geophys. Res. Atmos.*, **119**, 7889–7907, doi:10.1002/2014JD021478.
- , —, and —, 2015: Heavy precipitation in a changing climate: Does short-term summer precipitation increase faster? *Geophys. Res. Lett.*, **42**, 1165–1172, doi:10.1002/2014GL062588.
- Bechtold, P., J.-P. Chaboureaud, A. Beljaars, A. Betts, M. Köhler, M. Müller, and J.-L. Redelsperger, 2004: The simulation of the diurnal cycle of convective precipitation over land in a global model. *Quart. J. Roy. Meteor. Soc.*, **130**, 3119–3137, doi:10.1256/qj.03.103.

- Bénard, P., J. Vivoda, J. Mašek, P. Smolíková, K. Yessad, C. Smith, R. Brožková, and J.-F. Geleyn, 2010: Dynamical kernel of the Aladin–NH spectral limited-area model: Revised formulation and sensitivity experiments. *Quart. J. Roy. Meteor. Soc.*, **136**, 155–169, doi:10.1002/qj.522.
- Brockhaus, P., D. Lüthi, and C. Schär, 2008: Aspects of the diurnal cycle in a regional climate model. *Meteor. Z.*, **17**, 433–443, doi:10.1127/0941-2948/2008/0316.
- Chan, S. C., E. J. Kendon, H. J. Fowler, S. Blenkinsop, N. M. Roberts, and C. A. T. Ferro, 2014: The value of high-resolution Met Office regional climate models in the simulation of multihourly precipitation extremes. *J. Climate*, **27**, 6155–6174, doi:10.1175/JCLI-D-13-00723.1.
- Coles, S., 2001: *An Introduction to Statistical Modeling of Extreme Values*. Springer, 209 pp.
- Cuxart, J., P. Bougeault, and J.-L. Redelsperger, 2000: A turbulence scheme allowing for mesoscale and large eddy simulations. *Quart. J. Roy. Meteor. Soc.*, **126**, 1–30, doi:10.1002/qj.49712656202.
- Dai, A., 2006: Precipitation characteristics in eighteen coupled climate models. *J. Climate*, **19**, 4605–4630, doi:10.1175/JCLI3884.1.
- , and K. E. Trenberth, 2004: The diurnal cycle and its depiction in the community climate system model. *J. Climate*, **17**, 930–951, doi:10.1175/1520-0442(2004)017<0930:TDCAD>2.0.CO;2.
- Dee, D., and Coauthors, 2011: The ERA-Interim reanalysis: Configuration and performance of the data assimilation system. *Quart. J. Roy. Meteor. Soc.*, **137**, 553–597, doi:10.1002/qj.828.
- Doswell, C. A., H. E. Brooks, and R. A. Maddox, 1996: Flash flood forecasting: An ingredients-based methodology. *Wea. Forecasting*, **11**, 560–581, doi:10.1175/1520-0434(1996)011<0560:FFFAIB>2.0.CO;2.
- Ebert, E. E., and J. A. Curry, 1992: A parameterization of ice cloud optical properties for climate models. *J. Geophys. Res.*, **97**, 3831, doi:10.1029/91JD02472.
- Efron, B., and R. J. Tibshirani, 1993: *An Introduction to the Bootstrap*. Chapman and Hall, 456 pp.
- Feldmann, H., G. Schädler, H.-J. Panitz, and C. Kottmeier, 2013: Near future changes of extreme precipitation over complex terrain in central Europe derived from high resolution RCM ensemble simulations. *Int. J. Climatol.*, **33**, 1964–1977, doi:10.1002/joc.3564.
- Ferro, C. A. T., and J. Segers, 2003: Inference for clusters of extreme values. *J. Roy. Stat. Soc.*, **65**, 545–556, doi:10.1111/1467-9868.00401.
- Fosser, G., S. Khodayar, and P. Berg, 2015: Benefit of convection permitting climate model simulations in the representation of convective precipitation. *Climate Dyn.*, **44**, 45–60, doi:10.1007/s00382-014-2242-1.
- Fouquart, Y., and B. Bonnel, 1980: Computations of solar heating of the earth's atmosphere: A new parameterization. *Beitr. Phys. Atmos.*, **53**, 35–62.
- Frei, C., and C. Schär, 1998: A precipitation climatology of the Alps from high-resolution rain-gauge observations. *Int. J. Climatol.*, **18**, 873–900, doi:10.1002/(SICI)1097-0088(19980630)18:8<873::AID-JOC255>3.0.CO;2-9.
- , H. C. Davies, J. Gurtz, and C. Schär, 2000: Climate dynamics and extreme precipitation and flood events in central Europe. *Integr. Assess.*, **1**, 281–300, doi:10.1023/A:1018983226334.
- , R. Schöll, S. Fukutome, J. Schmidli, and P. Vidale, 2006: Future change of precipitation extremes in Europe: Intercomparison of scenarios from regional climate models. *J. Geophys. Res.*, **111**, D06105, doi:10.1029/2005JD005965.
- Früh, B., H. Feldmann, H.-J. Panitz, G. Schädler, D. Jacob, P. Lorenz, and K. Keuler, 2010: Determination of precipitation return values in complex terrain and their evaluation. *J. Climate*, **23**, 2257–2274, doi:10.1175/2009JCLI2685.1.
- Gao, X., Y. Xu, Z. Zhao, J. S. Pal, and F. Giorgi, 2006: On the role of resolution and topography in the simulation of East Asia precipitation. *Theor. Appl. Climatol.*, **86**, 173–185, doi:10.1007/s00704-005-0214-4.
- Gerard, L., 2007: An integrated package for subgrid convection, clouds and precipitation compatible with meso-gamma scales. *Quart. J. Roy. Meteor. Soc.*, **133**, 711–730, doi:10.1002/qj.58.
- , J.-M. Piriou, R. Brožková, J.-F. Geleyn, and D. Banciu, 2009: Cloud and precipitation parameterization in a meso-gamma-scale operational weather prediction model. *Mon. Wea. Rev.*, **137**, 3960–3977, doi:10.1175/2009MWR2750.1.
- Hohenegger, C., and B. Stevens, 2013: Controls on and impacts of the diurnal cycle of deep convective precipitation. *J. Adv. Model. Earth Syst.*, **5**, 801–815, doi:10.1002/2012MS000216.
- Hosking, J. R., 1990: L-moments: Analysis and estimation of distributions using linear combinations of order statistics. *J. Roy. Stat. Soc.*, **52**, 105–124.
- , and J. R. Wallis, 1987: Parameter and quantile estimation for the generalized pareto distribution. *Technometrics*, **29**, 339–349, doi:10.1080/00401706.1987.10488243.
- Isotta, F. A., and Coauthors, 2014: The climate of daily precipitation in the Alps: Development and analysis of a high-resolution grid dataset from pan-Alpine rain-gauge data. *Int. J. Climatol.*, **34**, 1657–1675, doi:10.1002/joc.3794.
- Kendon, E. J., N. M. Roberts, C. A. Senior, and M. J. Roberts, 2012: Realism of rainfall in a very high-resolution regional climate model. *J. Climate*, **25**, 5791–5806, doi:10.1175/JCLI-D-11-00562.1.
- , —, H. J. Fowler, M. J. Roberts, S. C. Chan, and C. A. Senior, 2014: Heavier summer downpours with climate change revealed by weather forecast resolution model. *Nat. Climate Change*, **4**, 570–576, doi:10.1038/nclimate2258.
- Kundzewicz, Z. W., and Coauthors, 2005: Summer floods in central Europe—Climate change track? *Nat. Hazards*, **36**, 165–189, doi:10.1007/s11069-004-4547-6.
- Lean, H. W., P. A. Clark, M. Dixon, N. M. Roberts, A. Fitch, R. Forbes, and C. Halliwell, 2008: Characteristics of high-resolution versions of the Met Office unified model for forecasting convection over the United Kingdom. *Mon. Wea. Rev.*, **136**, 3408–3424, doi:10.1175/2008MWR2332.1.
- Le Moigne, P., and Coauthors, 2012: Surfex scientific documentation. CNRM Tech. Rep., 237 pp. [Available online at http://www.cnrm-game-meteo.fr/surfex/IMG/pdf/surfex_scidoc_v2.pdf.]
- Lenderink, G., and E. van Meijgaard, 2010: Linking increases in hourly precipitation extremes to atmospheric temperature and moisture changes. *Environ. Res. Lett.*, **5**, 025208, doi:10.1088/1748-9326/5/2/025208.
- Liang, X.-Z., 2004: Regional climate model simulation of summer precipitation diurnal cycle over the United States. *Geophys. Res. Lett.*, **31**, L24208, doi:10.1029/2004GL021054.
- Lin, Y.-L., S. Chiao, T.-A. Wang, M. L. Kaplan, and R. P. Weglarz, 2001: Some common ingredients for heavy orographic rainfall. *Wea. Forecasting*, **16**, 633–660, doi:10.1175/1520-0434(2001)016<0633:SCIFHO>2.0.CO;2.
- Lindstedt, D., P. Lind, E. Kjellström, and C. Jones, 2015: A new regional climate model operating at the meso-gamma scale: Performance over Europe. *Tellus*, **67A**, 24138, doi:10.3402/tellusa.v67.24138.
- Louis, J., 1979: A parametric model of vertical eddy fluxes in the atmosphere. *Bound.-Layer Meteor.*, **17**, 187–202, doi:10.1007/BF00117978.

- Mašek, J., 2005: New parameterization of cloud optical properties proposed for model ALARO-0. Regional Cooperation for Limited Area Modeling in Central Europe Rep., 12 pp. [Available online at <http://www.rclace.eu/?page=74>.]
- Masson, V., and Coauthors, 2013: The SURFEXv7.2 land and ocean surface platform for coupled or offline simulation of Earth surface variables and fluxes. *Geosci. Model Dev.*, **6**, 929–960, doi:10.5194/gmd-6-929-2013.
- Mlawer, E. J., S. J. Taubman, P. D. Brown, M. J. Iacono, and S. A. Clough, 1997: Radiative transfer for inhomogeneous atmospheres: RRTM, a validated correlated-k model for the longwave. *J. Geophys. Res.*, **102**, 16 663–16 682, doi:10.1029/97JD00237.
- Molinari, J., and M. Dudek, 1992: Parameterization of convective precipitation in mesoscale numerical models: A critical review. *Mon. Wea. Rev.*, **120**, 326–344, doi:10.1175/1520-0493(1992)120<0326:POCPIM>2.0.CO;2.
- Morcrette, J.-J., and Y. Fouquart, 1986: The overlapping of cloud layers in shortwave radiation parameterizations. *J. Atmos. Sci.*, **43**, 321–328, doi:10.1175/1520-0469(1986)043<0321:TOOCLI>2.0.CO;2.
- Noilhan, J., and S. Planton, 1989: A simple parameterization of land surface processes for meteorological models. *Mon. Wea. Rev.*, **117**, 536–549, doi:10.1175/1520-0493(1989)117<0536:ASPOLS>2.0.CO;2.
- O’Gorman, P. A., and T. Schneider, 2009: The physical basis for increases in precipitation extremes in simulations of 21st-century climate change. *Proc. Natl. Acad. Sci. USA*, **106**, 14 773–14 777, doi:10.1073/pnas.0907610106.
- Pinty, J.-P., and P. Jabouille, 1998: Mixed-phase cloud parameterization for use in a mesoscale non-hydrostatic model: Simulations of a squall line and of orographic precipitation. *Proc. Conf. on Cloud Physics*, Everett, WA, Amer. Meteor. Soc., 217–220.
- Piriou, J.-M., J.-L. Redelsperger, J.-F. Geleyn, J.-P. Lafore, and F. Guichard, 2007: An approach for convective parameterization with memory: Separating microphysics and transport in grid-scale equations. *J. Atmos. Sci.*, **64**, 4127–4139, doi:10.1175/2007JAS2144.1.
- Prein, A. F., A. Gobiet, M. Suklitsch, H. Truhetz, N. K. Awan, K. Keuler, and G. Georgievski, 2013: Added value of convection permitting seasonal simulations. *Climate Dyn.*, **41**, 2655–2677, doi:10.1007/s00382-013-1744-6.
- , and Coauthors, 2015: A review on regional convection-permitting climate modeling: Demonstrations, prospects, and challenges. *Rev. Geophys.*, **53**, 323–361, doi:10.1002/2014RG000475.
- , and Coauthors, 2016: Precipitation in the EURO-CORDEX 0.11° and 0.44° simulations: High resolution, high benefits? *Climate Dyn.*, **46**, 383–412, doi:10.1007/s00382-015-2589-y.
- Rauscher, S. A., E. Coppola, C. Piani, and F. Giorgi, 2010: Resolution effects on regional climate model simulations of seasonal precipitation over Europe. *Climate Dyn.*, **35**, 685–711, doi:10.1007/s00382-009-0607-7.
- Ritter, B., and J. Geleyn, 1992: A comprehensive radiation scheme for numerical weather prediction models with potential applications in climate simulations. *Mon. Wea. Rev.*, **120**, 303–325, doi:10.1175/1520-0493(1992)120<0303:ACRSFN>2.0.CO;2.
- Roberts, N. M., and H. W. Lean, 2008: Scale-selective verification of rainfall accumulations from high-resolution forecasts of convective events. *Mon. Wea. Rev.*, **136**, 78–97, doi:10.1175/2007MWR2123.1.
- , S. J. Cole, R. M. Forbes, R. J. Moore, and D. Boswell, 2009: Use of high-resolution NWP rainfall and river flow forecasts for advance warning of the Carlisle flood, north-west England. *Meteor. Appl.*, **16**, 23–34, doi:10.1002/met.94.
- Rotunno, R., and R. Ferretti, 2001: Mechanisms of intense alpine rainfall. *J. Atmos. Sci.*, **58**, 1732–1749, doi:10.1175/1520-0469(2001)058<1732:MOIAR>2.0.CO;2.
- Rubel, F., and M. Hantel, 2001: Baltex 1/6-degree daily precipitation climatology 1996–1998. *Meteor. Atmos. Phys.*, **77**, 155–166, doi:10.1007/s007030170024.
- Ruiz-Villanueva, V., M. Borga, D. Zoccatelli, L. Marchi, E. Gaume, and U. Ehret, 2012: Extreme flood response to short-duration convective rainfall in south-west Germany. *Hydrol. Earth Syst. Sci.*, **16**, 1543–1559, doi:10.5194/hess-16-1543-2012.
- Seity, Y., P. Brousseau, S. Malardel, G. Hello, P. Bénard, F. Bouttier, C. Lac, and V. Masson, 2011: The AROME-France convective-scale operational model. *Mon. Wea. Rev.*, **139**, 976–991, doi:10.1175/2010MWR3425.1.
- Sharma, A., and H.-P. Huang, 2012: Regional climate simulation for Arizona: Impact of resolution on precipitation. *Adv. Meteor.*, **2012**, 505726, doi:10.1155/2012/505726.
- Tomassini, L., and D. Jacob, 2009: Spatial analysis of trends in extreme precipitation events in high-resolution climate model results and observations for Germany. *J. Geophys. Res.*, **114**, D12113, doi:10.1029/2008JD010652.
- Ulbrich, U., T. Brücher, A. H. Fink, G. C. Leckebusch, A. Krüger, and J. G. Pinto, 2003: The central European floods of August 2002: Part 2—Synoptic causes and considerations with respect to climatic change. *Weather*, **58**, 434–442, doi:10.1256/wea.61.03B.
- van den Besselaar, E. J. M., A. M. G. K. Tank, and T. A. Buishand, 2012: Trends in European precipitation extremes over 1951–2010. *Int. J. Climatol.*, **33**, 2682–2689, doi:10.1002/joc.3619.
- Walther, A., J.-H. Jeong, G. Nikulin, C. Jones, and D. Chen, 2013: Evaluation of the warm season diurnal cycle of precipitation over Sweden simulated by the Rossby Centre regional climate model RCA3. *Atmos. Res.*, **119**, 131–139, doi:10.1016/j.atmosres.2011.10.012.
- Weusthoff, T., F. Ament, M. Arpagaus, and M. W. Rotach, 2010: Assessing the benefits of convection-permitting models by neighborhood verification: Examples from MAP d-PHASE. *Mon. Wea. Rev.*, **138**, 3418–3433, doi:10.1175/2010MWR3380.1.
- Wüest, M., C. Frei, A. Altenhoff, M. Hagen, M. Litschi, and C. Schär, 2010: A gridded hourly precipitation dataset for Switzerland using rain-gauge analysis and radar-based disaggregation. *Int. J. Climatol.*, **30**, 1764–1775, doi:10.1002/joc.2025.